Severe Acute Respiratory Syndrome Coronavirus nsp1 Facilitates Efficient Propagation in Cells through a Specific Translational Shutoff of Host mRNA

Tomohisa Tanaka,[a] Wataru Kamitani,[a] Marta L. DeDiego,[c] Luis Enjuanes,[c] and Yoshiharu Matsuura[b]

Global COE Program[a] and Department of Molecular Virology,[b] Research Institute for Microbial Diseases, Osaka University, Osaka, Japan, and Department of Molecular and Cell Biology, Centro Nacional de Biotecnologia (CNB-CSIC), Campus Universidad Autonoma, Madrid, Spain[c]

Severe acute respiratory syndrome (SARS) coronavirus (SCoV) is an enveloped virus containing a single-stranded, positive-sense RNA genome. Nine mRNAs carrying a set of common 5′ and 3′ untranslated regions (UTR) are synthesized from the incoming viral genomic RNA in cells infected with SCoV. A nonstructural SCoV nsp1 protein causes a severe translational shutoff by binding to the 40S ribosomal subunits. The nsp1-40S ribosome complex further induces an endonucleolytic cleavage near the 5′UTR of host mRNA. However, the mechanism by which SCoV viral proteins are efficiently produced in infected cells in which host protein synthesis is impaired by nsp1 is unknown. In this study, we investigated the role of the viral UTRs in evasion of the nsp1-mediated shutoff. Luciferase activities were significantly suppressed in cells expressing nsp1 together with the mRNA carrying a luciferase gene, while nsp1 failed to suppress luciferase activities of the mRNA flanked by the 5′UTR of SCoV. An RNA-protein binding assay and RNA decay assay revealed that nsp1 bound to stem-loop 1 (SL1) in the 5′UTR of SCoV RNA and that the specific interaction with nsp1 stabilized the mRNA carrying SL1. Furthermore, experiments using an SCoV replicon system showed that the specific interaction enhanced the SCoV replication. The specific interaction of nsp1 with SL1 is an important strategy to facilitate efficient viral gene expression in infected cells, in which nsp1 suppresses host gene expression. Our data indicate a novel mechanism of viral gene expression control by nsp1 and give new insight into understanding the pathogenesis of SARS.

Severe acute respiratory syndrome (SARS) coronavirus (SCoV) is the etiological agent of a newly emerged disease, SARS, which originated in southern China in 2002 and spread worldwide in the 2003 epidemic (9, 17, 26). SCoV, which belongs to the genus *Betacoronavirus* in the family *Coronaviridae*, is an enveloped virus carrying a long (~27-kb), single-stranded, positive-sense genomic RNA. The 5′ two-thirds of SCoV genomic RNA, the gene 1 region, has two partially overlapping open reading frames (ORFs), 1a and 1b. Upon infection, the genomic RNA is translated to produce two large polyproteins and proteolytically processed into 16 mature viral proteins, nsp1 to nsp16, by two viral proteinases (27, 35). Most of the gene 1 proteins are essential for viral RNA synthesis, while some of them have other biological functions (3, 10, 21). Coronaviruses, including SCoV, use a unique strategy to produce a set of subgenomic mRNAs with common 5′ and 3′ sequences (35). Each mRNA contains a short 5′-terminal sequence (leader) derived from the 5′ end of the genome and a 3′-coterminal, nested-set structure. Like many host mRNAs, SCoV mRNAs are capped and polyadenylated, and the translation of viral mRNAs is thought to be cap dependent (4, 6, 8).

SCoV nsp1, the N-terminal protein coded by the gene 1, uses a two-pronged strategy to inhibit host gene expression by first binding to the 40S ribosomal subunit and then inactivating the translation activity of the 40S subunits (14). Ribosome-bound nsp1 further induces endonucleolytic RNA cleavage of a capped mRNA, rendering it translationally incompetent (13, 14). Importantly, nsp1 suppresses host innate immune responses by inhibiting type I interferon (IFN) expression in infected cells (23) and host antiviral signaling pathways (38). These data indicate that nsp1 plays important roles in SARS pathogenesis. Efficient SCoV gene expression occurs in the infected cells, in which nsp1 suppresses host gene expression (23), suggesting that SCoV escapes

from the nsp1-mediated gene expression suppression. Indeed, nsp1 does not induce endonucleolytic RNA cleavage of viral mRNAs in *in vitro* assays (13), implying that viral mRNAs are resistant to the nsp1-mediated RNA cleavage in infected cells. The mechanism by which SCoV mRNAs circumvent the nsp1-mediated gene expression suppression is unknown.

In this study, we show that interaction of nsp1 with stem-loop 1 (SL1) in the 5′ untranslated region (5′UTR) of SCoV RNAs confers resistance to the nsp1-mediated gene expression suppression and enhances viral RNA replication. Our data suggest that SCoV has evolved to protect its own mRNAs from the nsp1-mediated shutoff through a specific interaction of nsp1 with SL1 in the 5′UTR of the viral genome.

MATERIALS AND METHODS

Cells and transfection. 293T (human kidney) cell lines were maintained in Dulbecco's modified minimum essential medium (DMEM) (Sigma, St. Louis, MO) containing 10% fetal bovine serum (FBS), 100 U/ml penicillin, and 100 μg/ml streptomycin. All cells were cultured in a humidified 5% CO_2 atmosphere at 37°C. The plasmids were transfected into 293T cells or HeLa cells by using TransIT LT1 (Mirus, Madison, WI) according to the manufacturer's protocols. Bacterial artificial chromosome (BAC) constructs encoding SCoV replicon cDNA were transfected into 293T cells by using Lipofectamine 2000 (Invitrogen, Carlsbad, CA) as described

previously (1). Briefly, the cells were washed with DMEM three times before transfection. At 5 h posttransfection, the medium was replaced with fresh DMEM containing 10% FBS.

Plasmid constructions. The construction of the SCoV nsp1 expression plasmids, pCAG-nsp1-wt and pCAG-K164A/H165A (previously referred to as pCAGGS-Nsp1-WT and pCAGGS-Nsp1-mt, respectively), has been described elsewhere (23). The chloramphenicol acetyltransferase (CAT) ORF with a C-terminal myc tag sequence was cloned into pCAGGS-MCS, yielding pCAG-CAT. An inverse PCR procedure using pCAG-nsp1-wt as the template was employed to generate pCAG-K47A, pCAG-K58A, pCAG-R124A/K125A, pCAG-R124A, pCAG-K125A, pCAG-K164A, and pCAG-H165A. The firefly luciferase ORF was cloned into pcDNA3.1 HisA myc, yielding pcD-luc. Supernatants of Vero E6 cells infected with the SARS coronavirus, strain Frankfurt-1, in TRIzol reagent (Invitrogen) were kindly provided by Kazuyoshi Ikuta (Osaka University). Using a random hexamer, first-strand cDNA was prepared by using a avian myeloblastosis virus (AMV) reverse transcriptase first-strand cDNA synthesis kit (TaKaRa, Shiga, Japan) according to the manufacturer's instructions. The cDNA was used for the construction of the expression plasmid. The 5′UTR sequence of SCoV was connected downstream of the cytomegalovirus (CMV) promoter by overlapping PCR using the same method reported by Yamshchikov et al. (39), in which the CMV promoter-driven RNA transcripts have the precise 5′ terminus of SCoV RNA. The fragment was cloned between the CMV promoter and luciferase gene into pcD-luc, yielding pcD-5′luc. The 3′UTR of SCoV was cloned downstream of the luciferase gene into pcD-5′luc or pcD-luc, yielding pcD-5′luc3′ or pcD-luc3′, respectively. For mutational analysis of the nucleotide sequence from position 1 to 126 in the SCoV 5′UTR, a series of deletion mutants of 5′UTR was generated by using a KOD mutagenesis kit (Toyobo, Osaka, Japan) with pcD-5′luc as the template. The sequences of all of the constructs were confirmed with an ABI PRISM 3100 genetic analyzer (Applied Biosystems, Tokyo, Japan).

Luciferase assay. Luciferase activity was determined by using a luciferase assay system (Promega, Madison, WI) and an AB-2200 luminometer (Atto, Tokyo, Japan).

Northern blot analysis. Intracellular RNAs were prepared using Sepasol-RNA I SuperG reagent (Nacalai Tesque, Kyoto, Japan), electrophoresed through a 1% denaturing agarose gel using a formaldehyde-free RNA gel kit (Amresco, Cochran, OH), and then transferred onto a positively charged nylon membrane (Roche, Mannheim, Germany). Northern blot analysis was performed as described previously (15), and visualization was with a digoxigenin (DIG) luminescence detection kit (Roche).

Western blot analysis. Western blot analysis was performed as described previously (15). Mouse anti-myc antibody (Covance, Richmond, CA), mouse anti-actin antibody (Sigma, St. Louis, MO), rabbit anti-N antibody (Abcam, Cambridge, United Kingdom), and anti-nsp1 antibody were used as primary antibodies, and goat anti-mouse IgG–horseradish peroxidase (HRP) (Invitrogen) and goat anti-rabbit IgG–HRP (Invitrogen) were used as secondary antibodies.

Immunoprecipitation of reporter RNA. Immunoprecipitation of reporter RNAs was performed as described previously (24). 293T cells transfected with the indicated plasmids were lysed with lysis buffer (1% Triton X-100, 0.5% sodium deoxycholate, and 0.1% sodium dodecyl sulfate in phosphate-buffered saline) at 30 h posttransfection. The cell lysates were incubated with anti-myc antibody for 1 h at 4°C, and the immunoprecipitates were collected by centrifugation after incubation with protein A/G Plus-Agarose (Santa Cruz Biotechnology, Santa Cruz, CA) for 1 h at 4°C. The pellets were washed four times in lysis buffer, and RNAs were extracted by using Sepazol-RNA I Super G reagent (Nacalai Tesque). The extracted RNAs were subjected to Northern blot analysis.

RNA decay assay. Capped and polyadenylated CAT RNA and nsp1 RNA were synthesized by using a mMESSAGE mMACHINE T7 Ultra kit (Ambion, Austin, TX) as described previously (15). 293T cells transfected with 0.25 μg of either pcD-luc or pcD-5′luc were further transfected with

1 μg of either CAT RNA or nsp1 RNA at 24 h after primary transfection by using TransIT mRNA (Mirus) and then were treated with 4 μg/ml actinomycin D (ActD) (Sigma) at 1 h after RNA transfection for 8 h. Intracellular RNAs were extracted and subjected to Northern blot analysis.

BAC constructions. The construction of the SCoV-derived replicon, pBAC-wt (previously referred to as SARS-CoV-Rep), has been described elsewhere (1). pBAC-wt cDNA was digested with SfoI and MluI. This fragment was subcloned into a pSMART cloning vector, generating the plasmid pSMART-SARS1C. A QuikChange site-directed mutagenesis kit (Stratagene, La Jolla, CA) was used to generate a mutation (R124A) in nsp1 of the pSMART-SARS1C vector. The R124A-containing fragment was cloned back into pBAC-wt digested with SfoI and MluI, generating pBAC-R124A. To make the SCoV replicon expressing a *Renilla* luciferase reporter from subgenomic RNA, a *Renilla* luciferase (rluc) gene with a transcription-regulating sequence, which is required for synthesis of the subgenomic RNA of SCoV, was cloned into pBAC-wt and pBAC-R124A, generating pBAC-wt-rluc and pBAC-R124A-rluc, respectively.

RESULTS

The SCoV 5′UTR participates in evasion of nsp1-mediated shutoff and RNA degradation. To determine the effect of the UTRs of SCoV on circumventing the nsp1-mediated translational suppression, we constructed reporter plasmids carrying a firefly luciferase gene flanked by the 5′UTR and/or 3′UTR of SCoV (Fig. 1A) and cotransfected them into 293T cells with pCAG-nsp1-wt. As controls, pCAG-CAT, encoding chloramphenicol acetyltransferase (CAT), and pCAG-K164A/H165A, encoding a mutant nsp1 lacking the ability to suppress host translation and promote host RNA degradation by the replacement of K164 and H165 in the C-terminal region with alanines (23), were employed in place of pCAG-nsp1-wt. Consistent with previous data (23), the expression of nsp1-wt, but not that of K164A/H165A or CAT, suppressed luciferase expression in cells transfected with plasmid pcD-luc at 24 h posttransfection (Fig. 1B). However, luciferase expression in cells transfected with either pcD-5′luc3′ or pcD-5′luc abrogated the suppression by nsp1-wt, in contrast to the case in cells transfected with pcD-luc3′ (Fig. 1B). Similar results were also obtained in HeLa cells (data not shown) and by using another reporter plasmid, pcD-5′rluc, possessing the *Renilla* luciferase (rluc) gene under the 5′UTR of SCoV (Fig. 1E). These results suggest that the SCoV 5′UTR but not the 3′UTR plays an important role in circumventing the nsp1-mediated translational shutoff.
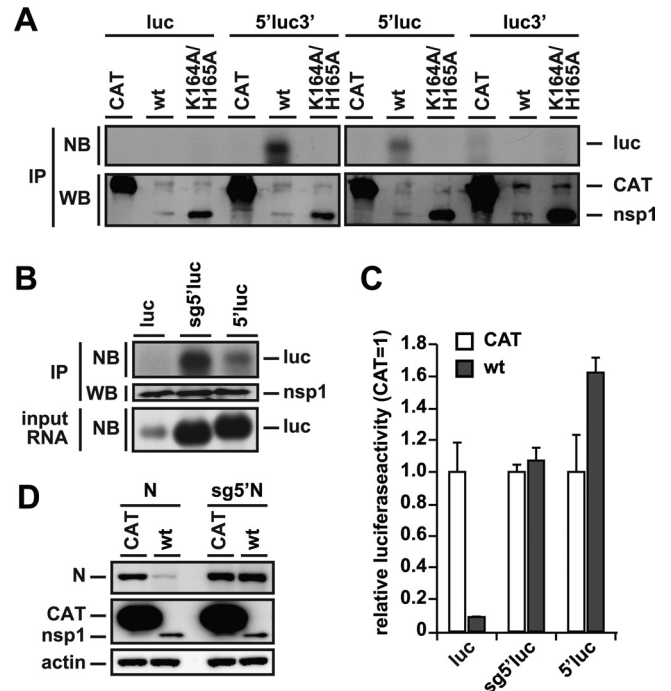
Next, to determine the effect of the 5′UTRs of SCoV on nsp1-mediated mRNA degradation, total RNAs extracted from 293T cells transfected with pcD-luc and pCAG-nsp1-wt were subjected to Northern blot analysis by using a specific probe for the luciferase gene. Consistent with previous reports (15, 23), the expression of nsp1-wt, but not that of K164A/H165A or CAT, decreased the amounts of luciferase mRNA at 24 h posttransfection (Fig. 1C). Interestingly, the amounts of luciferase mRNA in cells transfected with either pcD-5′luc3′ or pcD-5′luc were, rather, increased by the expression of nsp1-wt compared with those in cells transfected with either K164A/H165A or CAT (Fig. 1C), in spite of the similar expression levels of nsp1-wt among the samples (Fig. 1D). Similar results were also obtained in HeLa cells (data not shown). These results suggest that the SCoV 5′UTR has an ability to protect SCoV RNAs from nsp1-mediated RNA degradation.

Specific interaction of nsp1 with the 5′UTR of SCoV is required for evasion of nsp1-mediated gene suppression. To further examine the role of the SCoV 5′UTR in evasion of nsp1-
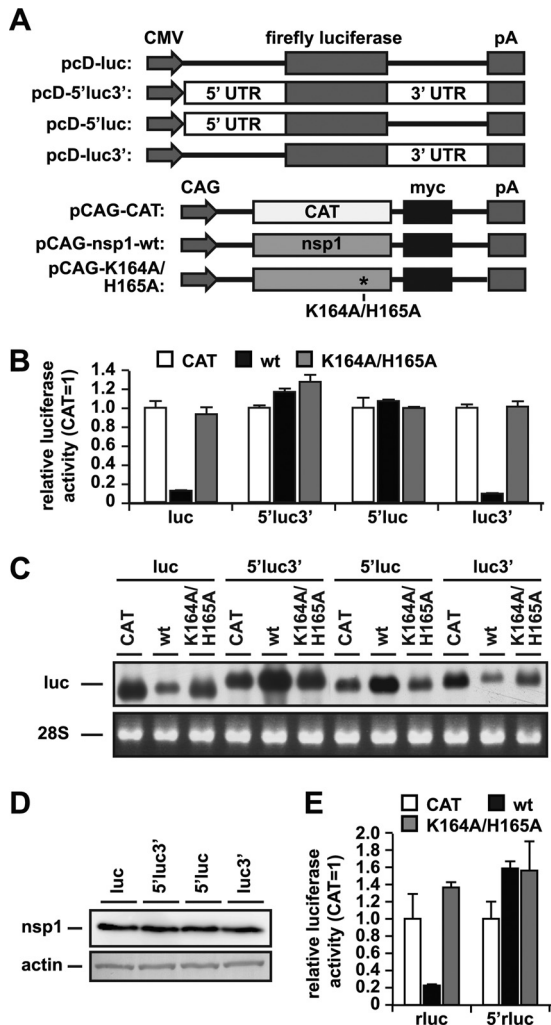
FIG 1 The SCoV 5′UTR participates in evasion of nsp1-mediated shutoff and RNA degradation. (A) Schematic diagrams of the reporter plasmids carrying the firefly luciferase (luc) gene with or without the 5′UTR and/or 3′UTR of SCoV under the control of the CMV promoter and of those carrying the nsp1 or chloramphenicol acetyltransferase (CAT) gene under the control of the CAG promoter. pA, polyadenylation signal. The asterisk represents the mutated amino acid position. (B) Luciferase activities in 293T cells transfected with 1 μg of either pCAG-nsp1-wt (wt), pCAG-K164A/H165A (K164A/H165A), or pCAG-CAT (CAT) together with 0.2 μg of the indicated reporter plasmids were determined at 24 h posttransfection after standardization with those in cells expressing CAT. The values represent the means ± standard deviations (SD) from three independent experiments. (C) Total RNAs prepared from the cells as shown in panel B were subjected to Northern blot analysis by using a riboprobe for the luciferase gene (luc). 28S rRNA was stained with ethidium bromide (28S). (D) Lysates of the cells as described in panel B were subjected to Western blot analysis using anti-myc and antiactin antibodies. (E) *Renilla* luciferase activities in 293T cells transfected with 0.5 μg of either pCAG-nsp1-wt (wt), pCAG-K164A/H165A (K164A/H165A), or pCAG-CAT (CAT) together with 0.1 μg of the indicated reporter plasmids encoding *Renilla* luciferase were determined at 24 h posttransfection after standardization with those in cells expressing CAT.
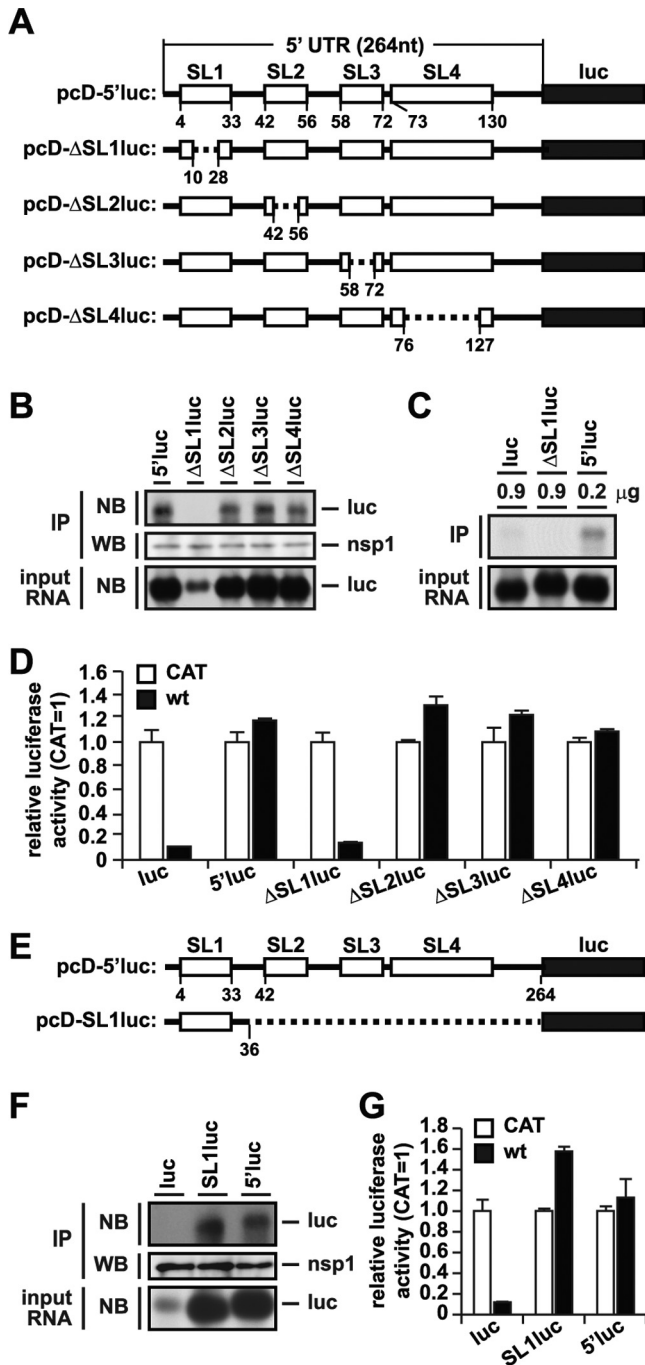
FIG 2 Specific interaction of nsp1 with the 5′UTR confers resistance to nsp1-mediated gene suppression. (A) Lysates of 293T cells transfected with 1 μg of either pCAG-nsp1-wt (wt), pCAG-K164A/H165A (K164A/H165A), or pCAG-CAT (CAT) together with 0.2 μg of the indicated reporter plasmids were immunoprecipitated with anti-myc antibody at 30 h posttransfection. RNAs extracted from the precipitates were subjected to Northern blot analysis using a riboprobe for the luciferase gene (NB). The precipitates were also subjected to Western blot analysis using anti-myc antibody (WB). (B) Lysates of 293T cells transfected with 1 μg of pCAG-nsp1-wt together with 0.2 μg of the indicated reporter plasmids were immunoprecipitated with anti-myc antibody at 30 h posttransfection. RNAs extracted from the precipitates were subjected to Northern blot analysis using a riboprobe for the luciferase gene (NB, top). The precipitates were also subjected to Western blot analysis using anti-myc antibody (WB). The bottom panel represents the amount of intracellular reporter RNAs in the lysates. (C) Luciferase activities in 293T cells transfected as described for panel B were determined at 24 h posttransfection after standardization with those in cells expressing CAT. The values represent the means ± SD from three independent experiments. (D) Lysates of 293T cells transfected with 1 μg of either pCAG-nsp1-wt (wt) or pCAG-CAT (CAT) together with 0.2 μg of either pcD-N (N) or pcD-sg5′N (sg5′N) were subjected to Western blot analysis by using either anti-N (top), anti-myc (middle), or anti-actin (bottom) antibody at 24 h posttransfection.

mediated gene suppression, we examined the interaction of nsp1 with the 5′UTR. Cells transfected with either pcD-luc, pcD-5′luc3′, pcD-5′luc, or pcD-luc3′ in combination with pCAG-nsp1-wt, pCAG-K164A/H165A, or pCAG-CAT were harvested at 24 h posttransfection and subjected to immunoprecipitation anal-

ysis by using anti-myc antibody; CAT and nsp1 proteins have a myc tag in the C terminus (Fig. 1A). Total RNAs were extracted from the immunoprecipitates and subjected to Northern blot analysis. Western blot analysis revealed that the expression of nsp1-wt was substantially lower than that of K164A/H165A or CAT (Fig. 2A), as nsp1 suppresses its own expression (15). The luciferase RNAs were coimmunoprecipitated with nsp1-wt but not with K164A/H165A or CAT in cells transfected with either pcD-5′luc3′ or pcD-5′luc but not in those transfected with pcD-luc or pcD-luc3′ (Fig. 2A), suggesting that nsp1 specifically interacts with the 5′UTR of SCoV.

SCoV utilizes a unique strategy to synthesize a set of subgenomic mRNAs that contain a common short 5′-terminal "leader" sequence derived from the 5′ end of the genome (35). To determine the interaction of nsp1 with the 5′UTR of subgenomic RNA, we generated pcD-sg5′luc by replacing the 5′UTR of pcD-

5'luc with that of subgenomic mRNA9 and transfected it into 293T cells together with pCAG-nsp1-wt. The mRNAs of both sg5'luc and 5'luc were coimmunoprecipitated with nsp1-wt (Fig. 2B, top). The amounts of immunoprecipitated nsp1-wt and lucif-erase RNAs in cells transfected with pcD-sg5'luc together with pCAG-nsp1-wt were comparable to those in cells transfected with pcD-5'luc together with pCAG-nsp1-wt (Fig. 2B, middle and bot-tom). Furthermore, the luciferase activity in cells transfected with either pcD-sg5'luc or pcD-5'luc, but not in those transfected with pcD-luc, was not decreased by the expression of nsp1-wt (Fig. 2C). These results suggest that SCoV escapes from the nsp1-mediated gene suppression through the interaction of nsp1 with both the genomic and subgenomic 5'UTRs of SCoV.

Next, to determine the role played by the interaction of nsp1 with the 5'UTR of SCoV in the expression of the viral protein, we constructed pcD-sg5'N, carrying the SCoV N gene in place of the luciferase gene in pcD-sg5'luc. Cells transfected with either pcD-sg5'N or pcD-N, which encodes the SCoV N gene under control of the CMV promoter, together with pCAG-nsp1-wt were harvested at 24 h posttransfection and subjected to Western blot analysis. As expected, expression of the N protein in cells coexpressing nsp1-wt upon transfection with pcD-sg5'N was not decreased, in contrast to the case in cells transfected with pcD-N (Fig. 2D). These results indicate that a specific interaction of nsp1 with the 5'UTR of SCoV plays an important role in the efficient expression of viral proteins in cells expressing nsp1.

Interaction of SL1 in the 5'UTR of SCoV with nsp1 is crucial for evasion of nsp1-mediated translational suppression. The 5'UTR of SCoV genomic RNA carries four major helical stem-loop (SL) structures, designated SL1 to SL4. The secondary struc-tures and sequences of the SLs in the 5'UTR of SCoV have been described in previous reports (5, 16). To determine the region(s) in the 5'UTR responsible for the specific interaction with nsp1, a series of SL deletion mutants based on pcD-5'luc were generated, as shown in Fig. 3A. The names and deleted nucleotide regions were as follows: pcD-ΔSL1luc, nucleotides (nt) 11 to 27; pcD-ΔSL2luc, nt 43 to 55; pcD-ΔSL3luc, nt 59 to 71; and pcD-ΔSL4luc, nt 77 to 126. Cells transfected with pCAG-nsp1-wt together with each of the SL deletion mutants were immunoprecipitated with anti-myc antibody at 24 h posttransfection, and total RNAs ex-tracted from the precipitates were subjected to Northern blot analysis. The 5'UTR of the subgenomic mRNA9 contains three SL structures (SL1, SL2, and SL3) (35, 40). Therefore, the sequence of

FIG 3 Interaction of SL1 in the 5'UTR of SCoV with nsp1 is crucial for evasion of nsp1-mediated translational suppression. (A) Schematic diagram of dele-tion mutants derived from the pcD-5'luc plasmid. White boxes, dashed lines, and black boxes indicate stem-loops (SL1, SL2, SL3, and SL4) in the 5'UTR, deletions, and the firefly luciferase gene (luc), respectively. The numbers indi-cate nucleotide positions. (B) Lysates of 293T cells transfected with 1 μg of pCAG-nsp1-wt together with 0.2 μg of the indicated reporter plasmids were immunoprecipitated with anti-myc antibody at 30 h posttransfection. RNAs extracted from the precipitates were subjected to Northern blot analysis using a riboprobe for the luciferase gene (NB, top). The precipitates were also sub-jected to Western blot analysis using anti-myc antibody (WB). The bottom panel represents the amount of intracellular reporter RNAs in the lysates. (C) 293T cells were transfected with 1 μg of pCAG-nsp1-wt together with either 0.9 μg of pcD-luc (luc), 0.9 μg of pcD-ΔSL1luc (ΔSL1luc), or 0.2 μg of pcD-5'luc (5'luc), and the cell extracts were immunoprecipitated by anti-myc

antibody. RNAs extracted from the precipitates were subjected to Northern blot analysis using a riboprobe for the luciferase gene (top). The bottom panel represents the amount of intracellular reporter RNAs in the lysates. (D) Lucif-erase activities in 293T cells transfected as described for panel B were deter-mined at 24 h posttransfection after standardization with those in cells ex-pressing CAT. The values represent the means ± SD from three independent experiments. (E) Schematic diagram of the pcD-SL1luc plasmid. Symbols are the same as in panel A. (F) Lysates of 293T cells transfected with 0.5 μg of pCAG-nsp1-wt together with 0.1 μg of the indicated reporter plasmids were immunoprecipitated with anti-myc antibody at 30 h posttransfection. RNAs extracted from the precipitates were subjected to Northern blot analysis using a riboprobe for the luciferase gene (NB, top). The precipitates were also sub-jected to Western blot analysis using anti-myc antibody (WB). The bottom panel represents the amount of intracellular reporter RNAs in the lysates. (G) Luciferase activities in 293T cells transfected as described for panel F were determined at 24 h posttransfection after standardization with those in cells expressing CAT. The values represent the means ± SD from three independent experiments.

the 5′UTR in pcD-ΔSL4luc was similar to that in pcD-sg5′luc. As we expected, ΔSL4luc RNA was efficiently coimmunoprecipitated with nsp1-wt (Fig. 3B, top). Furthermore, ΔSL2luc and ΔSL3luc RNAs, but not ΔSL1luc RNA, were coprecipitated with nsp1-wt (Fig. 3B, top). However, the intracellular expression of ΔSL1luc RNA was significantly lower than that of the other deletion constructs (Fig. 3B, bottom). To eliminate the possibility that the absence of coimmunoprecipitation of nsp1 with ΔSL1luc RNA was attributable to a low accumulation of ΔSL1luc RNA, we increased the amounts of transfected pcD-ΔSL1luc and found that no precipitation of ΔSL1luc RNA with nsp1-wt was observed even with the overexpression of the ΔSL1luc RNA (Fig. 3C). These results indicate that the SL1 in the 5′UTR of SCoV is responsible for a specific interaction with nsp1.

Next, to determine the effects of the SL region(s) on the nsp1-mediated translational suppression, luciferase expression in cells transfected with pCAG-nsp1-wt together with each of the SL deletion mutant plasmids, pcD-luc or pcD-5′luc, was determined at 24 h posttransfection. The expression of nsp1-wt suppressed the luciferase activities in cells transfected with pcD-ΔSL1luc or pcD-luc but not in those transfected with pcD-5′luc, pcD-ΔSL2luc, pcD-ΔSL3luc, or pcD-ΔSL4luc (Fig. 3D). These results indicate that SL1 in the 5′UTR of SCoV participates in evasion of nsp1-mediated translational suppression.

To further confirm the effect of SL1 on evasion of nsp1-mediated translational suppression, we constructed a pcD-SL1luc plasmid, containing SL1 in the region upstream of the luciferase gene (Fig. 3E). Both SL1luc RNA and 5′luc RNA were coimmunoprecipitated with nsp1-wt in cells transfected with either pcD-SL1luc or pcD-5′luc together with pCAG-nsp1-wt (Fig. 3F, top). In addition, no suppression of the luciferase expression was observed in cells transfected with either pcD-SL1luc or pcD-5′luc together with pCAG-nsp1-wt (Fig. 3G). These results confirm that the specific interaction of SL1 in the 5′UTR of SCoV with nsp1 is crucial for circumventing the nsp1-mediated translational suppression.

Interaction of the 5′UTR of SCoV with nsp1 through R124 is required for evasion of nsp1-mediated translational suppression. Structural analysis of SCoV nsp1 by nuclear magnetic resonance spectroscopy revealed the possibility that the positively charged region composed of K47, R124, and K125 on the surface is involved in the interaction with mRNA (2). To assess the interaction of the positively charged region in nsp1 with the 5′UTR of SCoV, we generated expression plasmids pCAG-K47A and pCAG-R124A/K125A, in which K47 and R124/K125 in nsp1, respectively, were replaced with alanine. As a control, pCAG-K58A, in which another positively charged residue, K58, on nsp1 was replaced with alanine, was employed. The expression levels of R124A/K125A and K47A were higher than those of nsp1-wt, while those of K58A were comparable to those of nsp1-wt (Fig. 4A). Nsp1 proteins were immunoprecipitated in cells transfected with either pCAG-nsp1-wt, pCAG-R124A/K125A, pCAG-K47A, or pCAG-K58A together with pcD-5′luc at 24 h posttransfection, and total RNAs extracted from the precipitates were subjected to Northern blot analysis. The luciferase RNAs containing the 5′UTR were coimmunoprecipitated with nsp1-wt, K47A, and K58A but not with R124A/K125A, suggesting that the positively charged amino acid residues R124 and/or K125 participate in the interaction with the 5′UTR of SCoV (Fig. 4B, top). To further determine the involvement of the R124 and K125 amino acid residues in the interaction with the 5′UTR, pCAG-R124A and
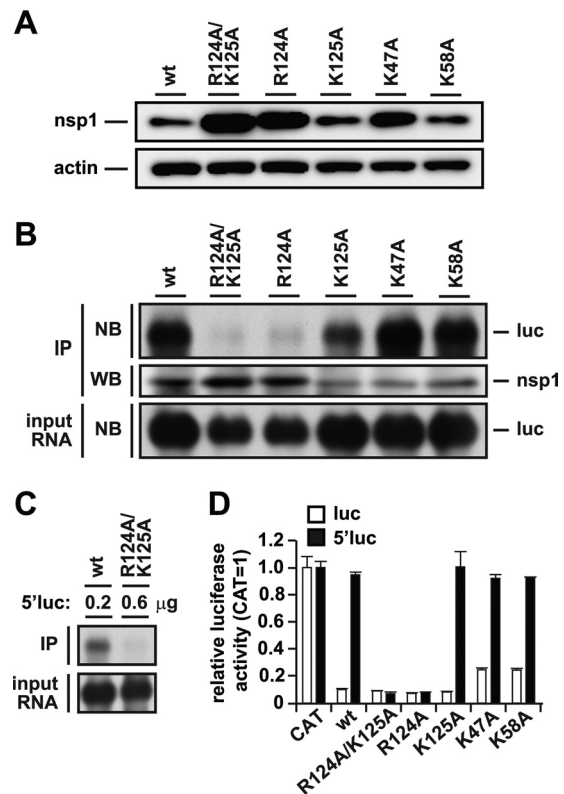
FIG 4 Interaction of the 5′UTR of SCoV with nsp1 through R124 is required for the evasion of the nsp1-mediated translational suppression. (A) Expression of nsp1 in 293T cells transfected with 1 μg of either pCAG-nsp1-wt (wt), pCAG-R124A/K125A (R124A/K125A), pCAG-R124A (R124A), pCAG-K125A (K125A), pCAG-K47A (K47A), or pCAG-K58A (K58A) was examined by Western blot analysis using anti-myc or anti-actin antibody at 24 h posttransfection. (B) Lysates of 293T cells transfected with 1 μg of each of the expression plasmids as described for panel A together with 0.2 μg of pcD-5′luc (5′luc) were immunoprecipitated with anti-myc antibody at 30 h posttransfection. RNAs extracted from the precipitates were subjected to Northern blot analysis using a riboprobe for the luciferase gene (NB, top). The precipitates were also subjected to Western blot analysis using anti-myc antibody (WB). The bottom panel represents the amount of intracellular reporter RNAs in the lysates. (C) 293T cells were transfected with 1 μg of either pCAG-nsp1-wt (wt) or pCAG-R124A/K125A (R124A/K125A) together with either 0.2 or 0.6 μg of pcD-5′luc, and cell extracts were immunoprecipitated with anti-myc antibody at 30 h posttransfection. RNAs extracted from the precipitates were subjected to Northern blot analysis using a riboprobe for the luciferase gene (top). The bottom panel represents the amount of intracellular reporter RNAs in the lysates. (D) Luciferase activities in 293T cells transfected with 0.5 μg of either expression plasmids as described for panel A or pCAG-CAT (CAT) together with 0.1 μg of either pcD-luc (luc) or pcD-5′luc (5′luc) were determined at 24 h posttransfection after standardization with those in cells expressing CAT. The values represent the means ± SD from three independent experiments.

pCAG-K125A, in which R124 and K125, respectively, were replaced with alanine, were generated. The luciferase RNAs carrying the 5′UTR were efficiently coimmunoprecipitated with K125A but not with R124A, in spite of the higher expression in R124A (Fig. 4B, top and middle). The amounts of luciferase RNA containing the 5′UTR of SCoV in cells expressing R124A or R124A/K125A were lower than those in cells expressing the wild type or K125A (Fig. 4B, bottom). To assess the interaction between the nsp1 mutants with comparable amounts of luciferase RNA, 3-fold-increasing amounts of pcD-5′luc (from 0.2 μg/well to 0.6 μg/well) were transfected, and similar levels of the luciferase RNA

were detected in both samples (Fig. 4C, bottom). However, no coprecipitation of the luciferase RNAs containing the 5′UTR with R124A/K125A was detected (Fig. 4C, top). These results suggest that a positively charged amino acid residue, R124, on the surface of nsp1 plays a crucial role in the interaction with the 5′UTR of SCoV.

Next, we determined the role of the positively charged residues in nsp1 in circumventing the nsp1-mediated translational suppression. The luciferase expression in cells transfected with each of the plasmids encoding nsp1 mutants together with either pcD-5′luc or pcD-luc was determined at 24 h posttransfection. The expression of the wild type and each of the mutants of nsp1, but not of CAT, exhibited a clear suppression of luciferase expression of pcD-luc, suggesting that all of the nsp1 mutants retained the ability to suppress the translation of mRNA lacking the 5′UTR of SCoV (Fig. 4D). In contrast, translational suppression of mRNA transcribed from pcD-5′luc containing the 5′UTR of SCoV was abrogated by the expression of the wild type, K125A, K47A, and K58A but not by the expression of R124A/K125A and R124A (Fig. 4D). These results suggested that the specific interaction of the 5′UTR of SCoV with nsp1 through R124A is required for circumventing the nsp1-mediated translational suppression.

Two functional domains in nsp1 participate in RNA binding and translational shutoff. The amino acid residue R124 in nsp1 was suggested to play a critical role in the interaction with the 5′UTR of SCoV, while K164A/H165A carrying a substitution of K164 and H165 with alanine but retaining R124 (23) failed to bind to the 5′UTR, as shown in Fig. 2A. To clarify this discrepancy, expression plasmids pCAG-K164A and pCAG-H165A, carrying a substitution of K164 and H165 in nsp1, respectively, with alanine, were generated (Fig. 5A). Cells transfected with either pCAG-CAT, pCAG-nsp1-wt, pCAG-K164A/H165A, pCAG-K164A, or pCAG-H165A together with pcD-5′luc were immunoprecipitated with anti-myc antibody at 24 h posttransfection, and total RNAs extracted from the immunoprecipitates were subjected to Northern blot analysis. Although the expression levels of K164A and H165A were lower than that of K164A/H165A (Fig. 5B), the 5′luc RNA was efficiently coprecipitated with K164A and H165A but not with K164A/H165A (Fig. 5C, top). Next, to determine the effects of the K164 and H165 mutations in nsp1 on the translational shutoff, luciferase activities in cells transfected with either pCAG-CAT, pCAG-nsp1-wt, pCAG-K164A/H165A, pCAG-K164A, or pCAG-H165A together with either pcD-luc or pcD-5′luc were determined at 24 h posttransfection. Although expression of K164A/H165A and K164A failed to suppress the luciferase expression of pcD-luc, that of H165A exhibited a suppression that was substantial but weaker than the suppression of nsp1-wt. Expression of the wild type and all of the mutant nsp1s exhibited no suppression of the luciferase expression of pcD-5′luc (Fig. 5D). These results suggest that nsp1 has at least two functional domains that are responsible for RNA binding and translational shutoff, respectively.

nsp1 enhances stability of RNA carrying the 5′UTR of SCoV. As described above, expression of the reporter RNA carrying the 5′UTR of SCoV was increased in cells expressing nsp1-wt (Fig. 1C), suggesting that binding of nsp1 specifically enhances the stability of the RNA possessing the 5′UTR. To assess this possibility, we performed an RNA decay assay as described previously (15). Cells transfected with either pcD-luc or pcD-5′luc were further transfected with each of the *in vitro*-transcribed RNAs carrying a
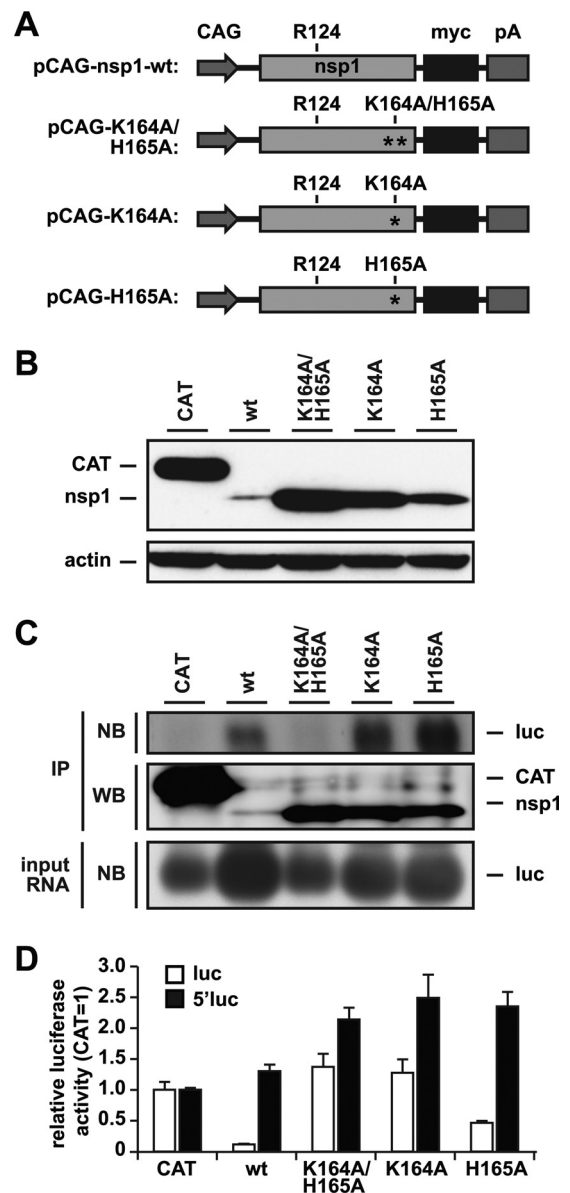
FIG 5 Two functional domains in nsp1 participate in RNA binding and translational shutoff. (A) Schematic diagrams of pCAG-nsp1-wt, pCAG-K164A/H165A, pCAG-K164A, and pCAG-H165A. CAG, CAG promoter; pA, polyadenylation signal. Asterisks represent the mutated amino acid position. (B) Expression of nsp1 in 293T cells transfected with 1 μg of either pCAG-nsp1-wt (wt), pCAG-K164A/H165A (K164A/H165A), pCAG-K164A (K164A), pCAG-H165A (H165A), or pCAG-CAT (CAT) was examined by Western blot analysis using anti-myc or antiactin antibody at 24 h posttransfection. (C) Lysates of 293T cells transfected with 1 μg of expression plasmids as described for panel A together with 0.2 μg of pcD-5′luc (5′luc) were immunoprecipitated with anti-myc antibody at 30 h posttransfection. RNAs extracted from the precipitates were subjected to Northern blot analysis using a riboprobe for luc (NB, top). The precipitates were also subjected to Western blot analysis using anti-myc antibody (WB). The bottom panel represents the amount of intracellular reporter RNAs in the lysates. (D) Luciferase activities in 293T cells transfected with 0.5 μg of either expression plasmids as described for panel A together with 0.1 μg of either pcD-luc (luc) or pcD-5′luc (5′luc) were determined at 24 h posttransfection after standardization with those in cells expressing CAT. The values represent the means ± SD from three independent experiments.
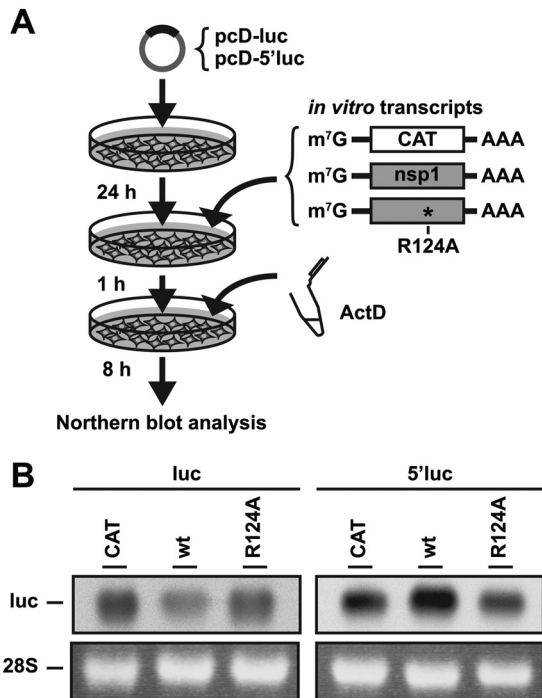
FIG 6 Nsp1 enhances the stability of RNA carrying the 5′UTR of SCoV. (A) Scheme for the RNA decay assay. 293T cells transfected with 0.25 μg of either pcD-luc (luc) or pcD-5′luc (5′luc) were further transfected with 1 μg each of RNAs carrying cap and poly(A) in the 5′ and 3′ ends, respectively, encoding either nsp1-wt, R124A, or CAT fused with myc-His tag in the C terminus at 24 h after primary transfection. Cells were further treated with 4 μg/ml of actinomycin D (ActD) at 1 h after RNA transfection, and intracellular RNAs were extracted at 8 h posttreatment and subjected to Northern blot analysis using a riboprobe for the luciferase gene. (B) Amounts of the luciferase RNA were examined by using Northern blot analysis (upper panels). 28S rRNA was stained with ethidium bromide (lower panels).

cap and poly(A) in the 5′ and 3′ ends, respectively, encoding either nsp1-wt, nsp1-R124A, or CAT, fused with the myc-His tag in the C terminus at 24 h after primary transfection. Cells were further treated with 4 μg/ml of actinomycin D (ActD) at 1 h after RNA transfection, and intracellular RNAs were extracted at 8 h post-treatment and subjected to Northern blot analysis (Fig. 6A). Consistent with previous studies (14, 23, 36), the amount of the luciferase RNA lacking the 5′UTR of SCoV was clearly decreased in cells expressing nsp1-wt in comparison with those expressing either R124A, which is incapable of binding to the 5′UTR of SCoV, or CAT. In contrast, the amount of the RNA possessing the 5′UTR of SCoV was increased in cells expressing nsp1-wt compared with those expressing either R124A or CAT (Fig. 6B). These results suggest that expression of nsp1-wt enhances the stability of RNA carrying the 5′UTR of SCoV through a specific interaction.

Specific interaction of nsp1 with the 5′UTR facilitates efficient replication of SCoV. To determine the biological significance of the interaction of nsp1 with the 5′UTR of SCoV for viral RNA replication, we employed an RNA replicon system in which SCoV RNA efficiently replicates but does not produce any infectious particles, based on a bacterial artificial chromosome (BAC), as described previously (1). We introduced an R124A mutation within the nsp1 gene of the parental SCoV replicon, pBAC-SARS-CoV-REP (pBAC-wt) to generate pBAC-R124A (Fig. 7A). Cells
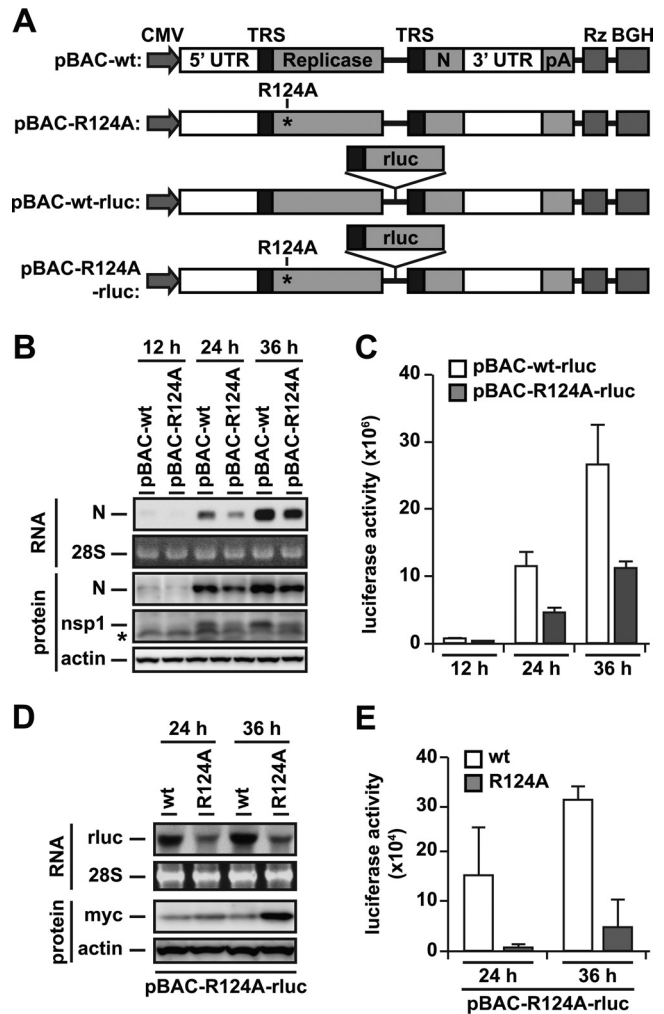
FIG 7 Specific interaction of nsp1 with the 5′UTR is required for efficient replication of SCoV. (A) Schematic diagram of cDNAs of the RNA replicon of SCoV. CMV, CMV promoter; TRS, transcription-regulatory sequence of SCoV; replicase, replicase gene of SCoV; pA, synthetic poly(A) tail; Rz, the self-cleaving ribozyme of hepatitis delta virus; BGH, BGH termination and polyadenylation signal. Asterisks represent the position of mutated amino acids. (B) 293T cells were transfected with 2.2 μg of either pBAC-wt or pBAC-R124As and the expression of viral RNA and proteins was determined at 12, 24, and 36 h posttransfection. Total RNAs extracted from the cells were subjected to Northern blot analysis using a riboprobe for the N gene. 28S rRNA was stained with ethidium bromide. Expression of N, nsp1, and actin was determined by Western blot analysis by using anti-N, anti-nsp1, and anti-actin antibody, respectively. The asterisk indicates a nonspecific signal. (C) Luciferase activities in 293T cells transfected with 1 μg of either pBAC-wt-rluc or pBAC-R124A-rluc were determined at 12, 24, and 36 h posttransfection. The values represent the means ± SD from three independent experiments. (D and E) 293T cells were transfected with 2.2 μg of pBAC-R124A-rluc together with 1 μg of either pCAG-nsp1-wt (wt) or pCAG-R124A (R124A), and the expression of viral RNA and proteins was determined at 24 and 36 h posttransfection. Total RNAs extracted from the cells were subjected to Northern blot analysis using a riboprobe for the *Renilla* luciferase gene (rluc). 28S rRNA was stained with ethidium bromide. Expression of nsp1 and actin was determined by Western blot analysis by using anti-myc and antiactin antibody, respectively. Luciferase activities in the cells were determined at 24 and 36 h posttransfection. The values represent the means ± SD from three independent experiments.

transfected with either pBAC-wt or pBAC-R124A were harvested at 12, 24, and 36 h posttransfection, and total RNA was extracted. Northern blot analysis using an N gene-specific probe revealed that the amounts of N mRNA in cells transfected with pBAC-R124A were significantly lower than those in cells transfected with pBAC-wt (Fig. 7B). Furthermore, the expression levels of both the N and nsp1 proteins were also lower in cells transfected with pBAC-R124A than in those transfected with pBAC-wt (Fig. 7B). To further confirm the impaired replication of the SCoV replicon carrying a mutation in R124, we inserted the rluc gene between the replicase and N genes with a transcription-regulatory sequence (TRS) of the N gene into pBAC-wt and pBAC-R124A, and generated pBAC-wt-rluc and pBAC-R124A-rluc, respectively (Fig. 7A); the TRS element, located upstream of each gene in the coronavirus genome, is required for subgenomic mRNA synthesis (31, 40). The levels of expression of rluc in cells transfected with either pBAC-wt-rluc or pBAC-R124A-rluc were determined at 12, 24, and 36 h posttransfection. As we expected, the luciferase activity in cells transfected with pBAC-R124A-rluc was approximately 50% lower than that in cells transfected with pBAC-wt-rluc (Fig. 7C).

Expression of nsp1 was shown to suppress the host antiviral response in cells infected with SCoV (23), and an nsp1 mutant in which R124 and K125 were replaced with serine and glutamine, respectively, partially lost its ability to inhibit the IFN signaling pathway (38). To assess the possibility that the lower level of replication of R124A-rluc RNA than of wt-rluc RNA was attributable to the deficiency in the suppression of the IFN signaling pathway, the expression of IFN-β mRNA was determined at 6, 12, 24, and 36 h posttransfection of the RNAs. However, no expression of IFN-β mRNA was induced in either wild-type or R124A-rluc replicon cells (data not shown), suggesting that the impaired replication of the R124A-rluc RNA replicon was not due to induction of an antiviral response.

To confirm the effect of the interaction of nsp1 with the 5′UTR of SCoV on viral replication, cells were transfected with pBAC-R124A-rluc together with either pCAG-nsp1-wt or pCAG-R124A, and then the replication of viral RNAs and expression of viral proteins were determined at 24 and 36 h posttransfection. Although the expression of nsp1-wt was significantly lower than that of R124A at 36 h posttransfection, replication of R124A-rluc RNA was significantly increased in cells expressing nsp1-wt (Fig. 7D). Furthermore, the luciferase expression in cells transfected with pBAC-R124A-rluc was also higher in cells expressing nsp1-wt than in those expressing R124A (Fig. 7E). These results suggest that a specific interaction of nsp1 with the 5′UTR of SCoV facilitates efficient viral replication.

DISCUSSION

Many RNA viruses have evolved to suppress host translation in order to promote virus-specific translation (22, 29). SCoV infection induces host translational shutoff (15, 23). Although many viral proteins that induce host translational shutoff are well characterized, SCoV nsp1 is the first viral protein that suppresses host gene expression by targeting the 40S ribosome. SCoV nsp1 inhibits host gene expression through interaction with the 40S ribosomal subunit, leading to translational suppression. The nsp1-40S ribosome complex modifies the 5′ regions of capped mRNA templates and renders them translationally incompetent (14). Although nsp1 induces endonucleolytic cleavage near the 5′UTR of the capped mRNA, SCoV is resistant to cleavage by nsp1. The

leader sequence located in the 5′ ends of all of the viral mRNAs as well as genomic RNA was shown to confer resistance to the nsp1-mediated endonucleolytic RNA cleavage in vitro (13). However, the precise mechanisms by which SCoV RNA resists the translational shutoff and RNA degradation induced by nsp1 are poorly understood. In this study, we have demonstrated that the specific interaction of nsp1 with the 5′UTRs of SCoV RNAs confers resistance to the nsp1-mediated translational shutoff and enhances viral RNA replication. Previous in vitro translation studies using HeLa cell extracts showed that nsp1 did not induce endonucleolytic RNA cleavage in viral mRNAs, but translation of mRNAs carrying either the 5′UTR or 3′UTR of SCoV was suppressed in the presence of recombinant nsp1 (13), in contrast to our present observation that the translation of mRNA carrying the 5′UTR but not the 3′UTR of SCoV leads to evasion of the nsp1-mediated translational shutoff. This discrepancy might be attributable to the lack of a host factor(s) essential for escape from the nsp1-mediated translational shutoff in the HeLa cell extracts. Further studies are needed to identify the molecule(s) responsible for ability of the mRNA carrying the 5′UTR of SCoV to circumvent nsp1-mediated gene silencing.

The positively charged region composed of K47, R124, and K125 on the surface of SCoV nsp1 has been suggested to be a putative RNA-binding site by nuclear magnetic resonance analysis (2). Bovine coronavirus (BCoV) nsp1 has also been shown to bind viral RNA and to regulate viral translation or replication (12). However, the target RNA(s) of the SCoV nsp1 has not been identified yet. In this study, we have shown that a positively charged amino acid residue, R124, on the surface of nsp1 is critical for the interaction with viral RNAs. Although the precise RNA-binding domain has not been identified in BCoV nsp1, the 8 amino acid residues (LRKxGxKG) conserved among betacoronavirus should participate in the RNA-binding activity of the nsp1 protein and exert a biological function in viral replication (2).

Previous reports have shown that the SL structures of coronavirus are required for RNA synthesis and gene expression (16, 19, 28). In the 5′UTR of mouse hepatitis virus (MHV), SL1 adopts a bipartite structure that drives a 5′UTR-3′UTR interaction and SL2 folds into a tetraloop structure that is required for subgenomic mRNA synthesis (18, 20). In this study, we have shown that SCoV SL1, located in both genomic and subgenomic viral RNAs, plays an important role in the viral replication through the interaction with nsp1. BCoV nsp1 binds to several cis-acting elements, especially in SL3 of the 5′UTR (12), while SCoV nsp1 binds only to SL1 in the 5′UTR, suggesting that the structure of SL1 in the 5′UTR of SCoV participates in the discrimination between viral (both genomic and subgenomic) RNAs and host mRNAs by the SCoV nsp1.

We also demonstrated that SCoV nsp1 is involved in the stabilization of viral RNAs, in contrast to the endonucleolytic cleavage of host mRNA. Although the precise mechanisms underlying the specific enhancement of the stability of RNA carrying the 5′UTR of SCoV by the expression of nsp1 remain unknown, this stabilization of genomic and subgenomic viral RNAs might contribute to the ability of the viral RNA to evade the nsp1-induced translational shutoff. The lack of any sequence homology with previously reported RNases suggests that nsp1 utilizes the host RNA decay machinery. Several mechanisms might explain why nsp1 specifically enhances the stabilization of viral RNA. Because the nsp1 mutant R124A, which was incapable of binding to SL1 in the

SCoV 5′UTR, failed to stabilize RNA carrying the sequence, the specific interaction of nsp1 with SL1 may participate in the evasion of the viral RNA from degradation by the host RNase. However, if nsp1 is still capable of binding to 40S ribosomes upon interaction with SL1, the translation of viral RNAs should be suppressed. Therefore, the interaction of nsp1 with SL1 may induce a conformational change in nsp1 to dissociate the 40S ribosome or recruit host factors to evade the nsp1-mediated shutoff. Several host factors, including hnRNP A1, hnRNP Q3, PTB, PABP, and MADP1, have been shown to interact with the UTRs of betacoronavirus (7, 19, 30, 32, 34). These host proteins have been shown to regulate the stability or translation of mRNA (11, 33), and therefore SCoV nsp1 may regulate their activities through the interaction with SL1 and enhance virus-specific translation. The hantavirus N protein has been shown to facilitate loading of the 43S preinitiation complex onto the viral RNA through binding with the 5′ cap structure, leading to efficient viral translation (25). Therefore, it might be speculated that interaction of nsp1 with SL1 induces recruitment of host factors to enhance viral translation. As shown in the nsp1 mutant R124A, which lacks the ability to bind to the 5′UTR, the interaction of nsp1 with SL1 was suggested to be required for evasion of RNA degradation; however, the nsp1 mutant K164A, which is able to bind to the 5′UTR, failed to suppress the nsp1-mediated translational shutoff, suggesting that SCoV nsp1 has two distinguishable functional domains responsible for RNA binding and translational shutoff, respectively.

In this study, we have shown that SCoV nsp1 enhances viral protein synthesis and RNA replication through the interaction with SL1 in the 5′UTR and that the mutant replicon RNA encoding the mutant nsp1 which is incapable of binding to the SL1 exhibited a low level of viral replication. A mutant SCoV carrying substitutions of R124 and K125 in nsp1 by serine and glutamine, respectively, failed to suppress host antiviral signaling pathways and exhibited impaired replication compared with the parental virus (38). The authors speculated that IFN induction upon infection with the mutant virus accounts for the impaired propagation, in contrast to our observation that IFN-β mRNA was not detectable in the replicon cells harboring the SCoV RNA carrying the nsp1 mutant R124A. Although the difference in amino acid substitutions might account for the discrepancy, expression of the nsp1 mutant R124A induced shutoff of the translation of host mRNAs, including the mRNAs of antiviral proteins, suggesting that the impaired replication of the SCoV replicon carrying the nsp1 mutant R124A is not due to IFN production.

Poliovirus virus 2Apro suppresses cap-dependent translation by cleavage of the N terminus of eIF4G, whereas translation of viral RNA takes place in a cap-independent manner through the internal ribosome entry site (IRES), which recruits the C-terminal fragment of eIF4G and the associated factors eIF4A and eIF3 (29). Rotavirus NSP3 also suppresses cap-dependent translation by disrupting the binding of eIF4G to PABP, whereas viral mRNA evades the translational suppression through the interaction of NSP3 with the 3′UTRs of viral mRNAs (37). Although SCoV nsp1 suppresses both cap-dependent and IRES-dependent translations (14), SCoV replicates efficiently in cells with impaired host protein synthesis by the expression of nsp1 through a specific interaction of nsp1 with the 5′UTRs of viral RNAs.

In conclusion, our data suggest that SCoV has evolved to protect its own mRNAs from the nsp1-mediated translational shutoff and RNA degradation through a specific interaction of nsp1 with the 5′UTR of the viral genome. This unique strategy for the translational shutoff by SCoV nsp1 should provide clues to the pathogenesis of SCoV and assist in the development of new therapeutic measures for SARS.

ACKNOWLEDGMENTS

REFERENCES

1. **Almazán F, et al.** 2006. Construction of a severe acute respiratory syndrome coronavirus infectious cDNA clone and a replicon to study coronavirus RNA synthesis. J. Virol. **80**:10900–10906.
2. **Almeida MS, Johnson MA, Herrmann T, Geralt M, Wüthrich K.** 2007. Novel beta-barrel fold in the nuclear magnetic resonance structure of the replicase nonstructural protein 1 from the severe acute respiratory syndrome coronavirus. J. Virol. **81**:3151–3161.
3. **Barretto N, et al.** 2005. The papain-like protease of severe acute respiratory syndrome coronavirus has deubiquitinating activity. J. Virol. **79**:15189–15198.
4. **Cencic R, et al.** 2011. Blocking eIF4E-eIF4G interaction as a strategy to impair coronavirus replication. J. Virol. **85**:6381–6389.
5. **Chen S, Olsthoorn R.** 2010. Group-specific structural features of the 5′-proximal sequences of coronavirus genomic RNAs. Virology **401**:29–41.
6. **Chen Y, et al.** 2011. Biochemical and structural insights into the mechanism of SARS coronavirus RNA ribose 2′-O-methylation by nsp16/nsp10 protein complex. PLoS Pathog. **7**:e1002294.
7. **Choi KS, Huang P, Lai MM.** 2002. Polypyrimidine-tract-binding protein affects transcription but not translation of mouse hepatitis virus RNA. Virology **303**:58–68.
8. **Decroly E, et al.** 2011. Crystal structure and functional analysis of the SARS-coronavirus RNA cap 2′-O-methyltransferase nsp10/nsp16 complex. PLoS Pathog. **7**:e1002059. doi:10.1371/journal.ppat.1002059.
9. **Drosten C, et al.** 2003. Identification of a novel coronavirus in patients with severe acute respiratory syndrome. N. Engl. J. Med. **348**:1967–1976.
10. **Graham RL, Sims AC, Brockway SM, Baric RS, Denison MR.** 2005. The nsp2 replicase proteins of murine hepatitis virus and severe acute respiratory syndrome coronavirus are dispensable for viral replication. J. Virol. **79**:13399–13411.
11. **Grosset C, et al.** 2000. A mechanism for translationally coupled mRNA turnover: interaction between the poly(A) tail and a c-fos RNA coding determinant via a protein complex. Cell **103**:29–40.
12. **Gustin K, Guan B, Dziduszko A, Brian D.** 2009. Bovine coronavirus nonstructural protein 1 (p28) is an RNA binding protein that binds terminal genomic cis-replication elements. J. Virol. **83**:6087–6097.
13. **Huang C, et al.** 2011. SARS coronavirus nsp1 protein induces template-dependent endonucleolytic cleavage of mRNAs: viral mRNAs are resistant to nsp1-induced RNA cleavage. PLoS Pathog. **7**:e1002433. doi:10.1371/journal.ppat.1002433.
14. **Kamitani W, Huang C, Narayanan K, Lokugamage KG, Makino S.** 2009. A two-pronged strategy to suppress host protein synthesis by SARS coronavirus Nsp1 protein. Nat. Struct. Mol. Biol. **16**:1134–1140.
15. **Kamitani W, et al.** 2006. Severe acute respiratory syndrome coronavirus nsp1 protein suppresses host gene expression by promoting host mRNA degradation. Proc. Natl. Acad. Sci. U. S. A. **103**:12885–12890.
16. **Kang H, Feng M, Schroeder M, Giedroc D, Leibowitz J.** 2006. Putative cis-acting stem-loops in the 5′ untranslated region of the severe acute respiratory syndrome coronavirus can substitute for their mouse hepatitis virus counterparts. J. Virol. **80**:10600–10614.

17. **Ksiazek TG, et al.** 2003. A novel coronavirus associated with severe acute respiratory syndrome. N. Engl. J. Med. **348**:1953–1966.

18. **Lee CW, Li L, Giedroc DP.** 2011. The solution structure of coronaviral stem-loop 2 (SL2) reveals a canonical CUYG tetraloop fold. FEBS Lett. **585**:1049–1053.

19. **Li HP, Zhang X, Duncan R, Comai L, Lai MM.** 1997. Heterogeneous nuclear ribonucleoprotein A1 binds to the transcription-regulatory region of mouse hepatitis virus RNA. Proc. Natl. Acad. Sci. U. S. A. **94**:9544–9549.

20. **Li L, et al.** 2008. Structural lability in stem-loop 1 drives a 5′ UTR-3′ UTR interaction in coronavirus replication. J. Mol. Biol. **377**:790–803.

21. **Lindner HA, et al.** 2005. The papain-like protease from the severe acute respiratory syndrome coronavirus is a deubiquitinating enzyme. J. Virol. **79**:15199–15208.

22. **Lloyd RE.** 2006. Translational control by viral proteinases. Virus Res. **119**:76–88.

23. **Narayanan K, et al.** 2008. Severe acute respiratory syndrome coronavirus nsp1 suppresses host gene expression, including that of type I interferon, in infected cells. J. Virol. **82**:4471–4479.

24. **Narayanan K, Maeda A, Maeda J, Makino S.** 2000. Characterization of the coronavirus M protein and nucleocapsid interaction in infected cells. J. Virol. **74**:8127–8134.

25. **Panganiban AT, Mir MA.** 2009. Bunyavirus N: eIF4F surrogate and cap-guardian. Cell Cycle **8**:1332–1337.

26. **Poutanen SM, et al.** 2003. Identification of severe acute respiratory syndrome in Canada. N. Engl. J. Med. **348**:1995–2005.

27. **Prentice E, McAuliffe J, Lu XT, Subbarao K, Denison MR.** 2004. Identification and characterization of severe acute respiratory syndrome coronavirus replicase proteins. J. Virol. **78**:9977–9986.

28. **Raman S, Bouma P, Williams GD, Brian DA.** 2003. Stem-loop III in the 5′ untranslated region is a cis-acting element in bovine coronavirus defective interfering RNA replication. J. Virol. **77**:6720–6730.

29. **Schneider RJ, Mohr I.** 2003. Translation initiation and viral tricks. Trends Biochem. Sci. **28**:130–136.

30. **Shi ST, Huang PY, Li HP, Lai MMC.** 2000. Heterogeneous nuclear ribonucleoprotein A1 regulates RNA synthesis of a cytoplasmic virus. EMBO J. **19**:4701–4711.

31. **Sola I, Moreno JL, Zuniga S, Alonso S, Enjuanes L.** 2005. Role of nucleotides immediately flanking the transcription-regulating sequence core in coronavirus subgenomic mRNA synthesis. J. Virol. **79**:2506–2516.

32. **Spagnolo JF, Hogue BG.** 2000. Host protein interactions with the 3′ end of bovine coronavirus RNA and the requirement of the poly(A) tail for coronavirus defective genome replication. J. Virol. **74**:5053–5065.

33. **Svitkin YV, Ovchinnikov LP, Dreyfuss G, Sonenberg N.** 1996. General RNA binding proteins render translation cap dependent. EMBO J. **15**:7147–7155.

34. **Tan YW, Hong W, Liu DX.** 2012. Binding of the 5′-untranslated region of coronavirus RNA to zinc finger CCHC-type and RNA-binding motif 1 enhances viral replication and transcription. Nucleic Acids Res. **40**:5065–5077.

35. **Thiel V, et al.** 2003. Mechanisms and enzymes involved in SARS coronavirus genome expression. J. Gen. Virol. **84**:2305–2315.

36. **Tohya Y, et al.** 2009. Suppression of host gene expression by nsp1 proteins of group 2 bat coronaviruses. J. Virol. **83**:5282–5288.

37. **Vende P, Piron M, Castagne N, Poncet D.** 2000. Efficient translation of rotavirus mRNA requires simultaneous interaction of NSP3 with the eukaryotic translation initiation factor eIF4G and the mRNA 3′ end. J. Virol. **74**:7064–7071.

38. **Wathelet MG, Orr M, Frieman MB, Baric RS.** 2007. Severe acute respiratory syndrome coronavirus evades antiviral signaling: role of nsp1 and rational design of an attenuated strain. J. Virol. **81**:11620–11633.

39. **Yamshchikov V, Mishin V, Cominelli F.** 2001. A new strategy in design of (+)RNA virus infectious clones enabling their stable propagation in E coli. Virology **281**:272–280.

40. **Zúñiga S, Sola I, Alonso S, Enjuanes L.** 2004. Sequence motifs involved in the regulation of discontinuous coronavirus subgenomic RNA synthesis. J. Virol. **78**:980–994.